LARGE, an intellectual disability-associated protein, regulates AMPA-type glutamate receptor trafficking and memory

Bo Am Seo[a,b], Taesup Cho[a], Daniel Z. Lee[c], Joong-jae Lee[a], Boyoung Lee[a], Seong-Wook Kim[a], Hee-Sup Shin[a,1], and Myoung-Goo Kang[a,b,c,1]

[a]Center for Cognition and Sociality, Institute for Basic Science, 34141 Daejeon, Republic of Korea; [b]Biomedical Science & Engineering Interdisciplinary Program, Korea Advanced Institute of Science and Technology, 34141 Daejeon, Republic of Korea; and [c]Department of Neuroscience and Cell Biology, University of Texas Medical Branch, Galveston, TX 77555

Contributed by Hee-Sup Shin, May 24, 2018 (sent for review March 23, 2018; reviewed by Richard L. Huganir and Mu-ming Poo)

Mutations in the human LARGE gene result in severe intellectual disability and muscular dystrophy. How *LARGE* mutation leads to intellectual disability, however, is unclear. In our proteomic study, LARGE was found to be a component of the AMPA-type glutamate receptor (AMPA-R) protein complex, a main player for learning and memory in the brain. Here, our functional study of LARGE showed that LARGE at the Golgi apparatus (Golgi) negatively controlled AMPA-R trafficking from the Golgi to the plasma membrane, leading to down-regulated surface and synaptic AMPA-R targeting. In *LARGE* knockdown mice, long-term potentiation (LTP) was occluded by synaptic AMPA-R overloading, resulting in impaired contextual fear memory. These findings indicate that the fine-tuning of AMPA-R trafficking by LARGE at the Golgi is critical for hippocampus-dependent memory in the brain. Our study thus provides insights into the pathophysiology underlying cognitive deficits in brain disorders associated with intellectual disability.

intellectual disability | synaptic plasticity | AMPA receptor | LARGE

LARGE gene is expressed strongly in the brain (particularly the hippocampus) relative to other tissues (1). In humans, mutations in *LARGE* are associated with congenital muscular dystrophy type 1D, which is characterized by clinical features that include profound intellectual disability, abnormal electroretinogram findings, and subtle structural brain abnormalities (2–5). *Large*^{myd} mice, which carry a natural truncation mutation of *LARGE*, exhibit a number of neurological phenotypes, including sensorineural deafness and defective retinal transmission, along with developmental brain abnormalities (6, 7) and impaired long-term potentiation (LTP) (8). These human and mouse studies suggest that abnormal synaptic function may be responsible for intellectual disabilities in human patients with *LARGE* mutations.

In our previous proteomic analysis, we found that LARGE forms a protein complex with the AMPA-type glutamate receptor (AMPA-R) (9). Excitatory glutamatergic synaptic transmission within the central nervous system is primarily mediated by AMPA-R, as well as NMDA-type glutamate receptor (NMDA-R), and increasing numbers of proteins have been found to form complexes with, and thus regulate, the dynamic trafficking of AMPA-R. This tight regulation of AMPA-R trafficking in and out of the synapses, mediated by AMPA-R interactors, is widely considered to be a central brain mechanism involved in information storage (10).

In the present study, LARGE down-regulated the synaptic targeting of AMPA-R by negatively modulating AMPA-R trafficking from the Golgi apparatus (Golgi) to the cell surface. Synaptic AMPA-R overloading due to LARGE deficiency causes hippocampal LTP occlusion. Both knockout (KO; *Large*$^{myd-/-}$) and knockdown (KD) animals stereotaxically injected with a virus carrying small hairpin RNA (shRNA) targeting LARGE exhibited deficits in associative fear memory. Taken together, LARGE plays a critical role in memory by tuning the synaptic targeting of AMPA-R in the hippocampus. Our findings thus suggest that the abnormal trafficking of AMPA-R underlies cognitive deficits observed in patients with LARGE gene mutations.

Results

LARGE Up-Regulates the Golgi Localization of AMPA-R. LARGE is known to localize at the Golgi in heterologous cells (11) and to function at the Golgi in myocytes (12). Similarly, in cultured hippocampal neurons, we observed a major pool of LARGE at the Golgi and Golgi outposts (Fig. 1*A*). Next, we analyzed the colocalization of GluA1, a subunit of AMPA-R, with the Golgi marker GM130 in cultured hippocampal neurons after manipulating LARGE expression using *LARGE* shRNA or *LARGE* rescue cDNA. The efficacy of shRNA-mediated *LARGE* KD and rescue was validated (*SI Appendix*, Fig. S1). Confocal imaging demonstrated that *LARGE* KD significantly decreased the pool of GluA1 at the Golgi, whereas *LARGE* rescue reversed this phenomenon (Fig. 1*B*). Similarly, in HEK293T cells, LARGE overexpression significantly increased AMPA-R localization at the Golgi (*SI Appendix*, Fig. S2*A*).

We also biochemically analyzed the effects of LARGE coexpression on subcellular AMPA-R localization by fractionating subcellular organelles from HEK293T cells transfected with GluA1 without (−LRG) or with (+LRG) LARGE (Fig. 1*C*).

Significance

In human patients, mutations in the *LARGE* gene cause congenital muscular dystrophy (CMD) type 1D, which, unlike other types of CMD, is accompanied by severe intellectual disability. Neurological phenotypes of *LARGE* knockout mice also suggest the possibility of impaired learning and memory. Our study using region-specific *LARGE* knockdown provides strong evidence that a deficit of LARGE in the hippocampus results in excitatory synapses being abnormally potentiated through the overloading of AMPA-type glutamate receptor, thereby impairing hippocampus-dependent memory. Our data reveal an intriguing role for LARGE in regulating the fine-tuning of synaptic strength in the hippocampus, which influences hippocampus-dependent memory. The results provide crucial insights for the therapeutic treatment of brain disorders associated with intellectual disability.

Author contributions: H.-S.S. and M.-G.K. designed research; B.A.S., T.C., D.Z.L., J.-j.L., B.L., S.-W.K., H.-S.S., and M.-G.K. performed research; B.A.S., T.C., D.Z.L., J.-j.L., B.L., S.-W.K., H.-S.S., and M.-G.K. analyzed data; and B.A.S., H.-S.S., and M.-G.K. wrote the paper.

Reviewers: R.L.H., The Johns Hopkins University School of Medicine; and M.-m.P., Chinese Academy of Sciences.

The authors declare no conflict of interest.

[1]To whom correspondence may be addressed. Email: shin@ibs.re.kr or mkang13@gmail.com.

This article contains supporting information online at www.pnas.org/lookup/suppl/doi:10.1073/pnas.1805060115/-/DCSupplemental.

Published online June 18, 2018.

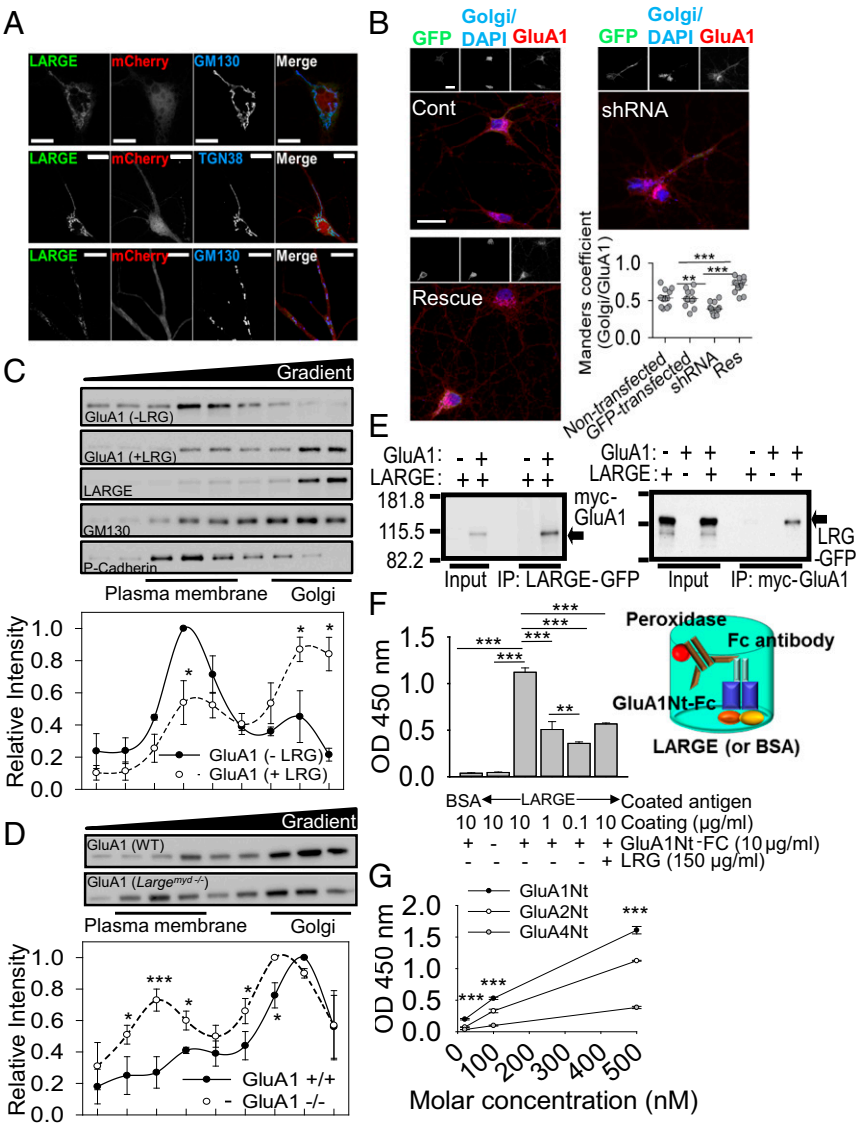

Fig. 1. LARGE directly interacted with AMPA-R to increase AMPA-R localization at the Golgi. (*A*) Confocal images demonstrating major pools of GFP-tagged LARGE in the *cis*-Golgi (*Top*, marked by TGN38), *trans*-Golgi (*Middle*, marked by TGN38), and Golgi outposts (*Bottom*) of cultured hippocampal neurons. (Scale bars: 10 μm.) (*B*) *LARGE* KD (shRNA) decreased GluA1 at the Golgi, compared with non-transfected and scrambled shRNA-transfected neurons (Cont), which was reversed by *LARGE* rescue (Res) ($n = 12$ neurons, $n = 11$ neurons, $n = 12$ neurons, $n = 13$ neurons; $^{**}P < 0.01$, $^{***}P < 0.001$). (Scale bars: 30 μm.) (*C*) Density gradient-based subcellular fractionation of HEK293T cells. By the coexpression of LARGE with GluA1 (+LRG), the relative size of the GluA1 pool at the Golgi (GM130) increased significantly, whereas that in the plasma membrane (P-Cadherin) decreased significantly relative to the control group (–LRG, GluA1 only) ($n = 3$; two-tailed *t* test: $^{*}P < 0.05$). (*D*) Subcellular fractionation of hippocampi from *LARGE* KO mice ($Large^{myd-/-}$) revealed relative decreases and increases, respectively, in the relative sizes of the GluA1 pools in the Golgi and plasma membrane, compared with those in wild-type mice (WT) ($n = 3$, three mice; two-tailed *t* test: $^{*}P < 0.05$, $^{***}P < 0.001$). (*E*) LARGE-GFP (LRG-GFP) had been coexpressed with myc-tagged GluA1 (myc-GluA1) in HEK293T cells. Immunoprecipitation (IP) of LARGE with an anti-GFP antibody specifically coimmunoprecipitated GluA1 (*Left*), and IP of GluA1 with an anti-myc antibody specifically coimmunoprecipitated LARGE (*Right*). (*F*) Direct interaction between LARGE and AMPA-R was examined using an ELISA. The LARGE ectodomain used to coat the bottom of the plate bound directly to the Fc-fused N-terminal ectodomain of GluA1 (GluA1Nt-Fc). Binding was quantified by measuring the activity of FC antibody-coupled peroxidase ($n = 3$; $^{**}P < 0.01$, $^{***}P < 0.001$). (*G*) Another ELISA used to evaluate the relative binding affinities of LARGE for each AMPA-R subunit yielded the following order: GluA1 > GluA2 > GluA4 ($n = 3$; $^{***}P < 0.001$ compared with GluA2 and GluA4). One-way ANOVA (*B* and *F*) and two-way repeated measure ANOVA (*G*) were used.

Without LARGE coexpression, the major GluA1 pool was detected in fractions enriched for P-cadherin, a plasma membrane marker. With LARGE coexpression, however, the major GluA1 pool shifted to high-density fractions enriched for GM130, a Golgi marker. Furthermore, the distributions of GluA1 and LARGE in the gradient almost completely overlapped when the proteins were coexpressed (Fig. 1*C*), indicating a strong and direct association. Moreover, the relative AMPA-R pool size in the Golgi fractions decreased significantly in the brains of *LARGE* KO mice relative to wild-type mice, whereas the relative pool size in the plasma membrane fractions increased significantly (Fig. 1*D* and *SI Appendix*, Fig. S2*B*). These results suggest that LARGE plays an important role in maintaining AMPA-R pools at the Golgi.

LARGE Associates with AMPA-R Through Direct Interaction. HEK293T cells do not express synaptic proteins. Therefore, the cosedimentation and colocalization of GluA1 with LARGE in these cells (Fig. 1*B* and *SI Appendix*, Fig. S2*A*) suggested a direct interaction. To test this possibility, we performed reciprocal coimmunoprecipitation (co-IP) of LARGE and AMPA-R from HEK293T cells. Both co-IP strategies consistently showed that LARGE could specifically bind to AMPA-R in nonneuronal cells that do not express other known AMPA-R–binding proteins (Fig. 1*E*). Interestingly, in co-IP of LARGE with GluA2, LARGE binding only to the GluA2 corresponded to intracellular GluA2 (13) (*SI Appendix*, Fig. S3*A*), suggesting that LARGE binds with AMPA-R within the cell, likely at the Golgi.

We further reconstituted the interaction of LARGE with AMPA-R in vitro using an ELISA (Fig. 1 *F* and *G*). Given the molecular structures and topologies of LARGE and GluA1, we hypothesized that the C-terminal ectodomain of LARGE would bind the N-terminal ectodomain of GluA1. After confirming the purification of each protein (*SI Appendix*, Fig. S3 *B–E*), we constructed an ELISA to verify the specific and direct interaction of LARGE with GluA1 (Fig. 1 *F* and *G*). Notably, GluA1 bound to LARGE with a higher affinity relative to that exhibited by GluA2 or GluA4 (Fig. 1*G*).

As GluA1 binds directly to the LARGE ectodomain (including catalytic domains), we evaluated whether the interaction of LARGE with AMPA-R could affect glycosylation of the latter. However, we observed no dramatic changes in LARGE-mediated GluA1 glycosylation (*SI Appendix*, Fig. S4), suggesting that the physical interaction of LARGE with GluA1, rather than LARGE glycosyltransferase activity, is the essential element with respect to AMPA-R. Similarly, a previous report found that the physical interaction of Notch with OFUT1, a glycosyltransferase, rather than OFUT1 enzymatic activity, was essential to the role of OFUT1 in Notch trafficking (14).

LARGE Down-Regulates AMPA-R Surface Localization. Our results (Fig. 1 and *SI Appendix*, Figs. S2 and S3) consistently demonstrate the ability of LARGE to interact directly and specifically with AMPA-R to increase localization of the latter protein at the Golgi, which suggests that LARGE could down-regulate the cell-surface localization of AMPA-R. Indeed, our surface biotinylation approach demonstrated significant increases and decreases in AMPA-R surface localization in response to *LARGE* KD and rescue, respectively, whereas KD or rescue did not affect total AMPA-R expression or NMDA-R surface localization (Fig. 2*A*). We additionally evaluated AMPA-R surface localization ex vivo using membrane-impermeable bis(sulfosuccinimidyl) suberate, which cross-links proteins exposed on the cell surface (Fig. 2*B*). The molecular mass of cross-linked surface GluA1 (>250 kDa) was higher than that of intracellular GluA1 (~105 kDa), consistent with our previous study (15). Although the surface and intracellular GluA1 levels, respectively, increased and decreased significantly in $Large^{myd-/-}$ mice relative to wild-type mice, NMDA-R surface localization was not affected by LARGE deficiency (Fig. 2*B*), further confirming that LARGE specifically modulates AMPA-R. The increased AMPA-R surface localization following *LARGE* KD was also confirmed at the single-cell level (Fig. 2*C*).

We further investigated whether LARGE could modulate AMPA-R surface localization in a heterologous expression system. Here, in HEK293T cell culture, LARGE overexpression led to strong decreases in surface GluA1 and GluA2 localization but did not affect total AMPA-R expression (Fig. 2*D*). The observed greater decrease in GluA1 relative to GluA2 (Fig. 2*D*) may be explained by the lower binding of LARGE with GluA2 compared with that with GluA1 in the ELISA (Fig. 1*G*). Again, the effect of LARGE overexpression on AMPA-R surface localization was recapitulated in individual hippocampal neurons (Fig. 2*E*).

***LARGE* KD Impairs Hippocampal LTP due to Postsynaptic AMPA-R Overload.** The regulation of AMPA-R trafficking by LARGE suggests a potential role of this protein in synaptic plasticity, which has been proposed by previous studies of LARGE (1–8), including LTP analysis (8). The LTP deficit in *LARGE* KO mice could be due to abnormal brain development, such as a neuronal migration defect (6, 8). To determine whether LARGE could affect synaptic plasticity in the normally developed adult mouse brain, we investigated hippocampal synaptic plasticity via in vivo LTP after KD of LARGE after the stereotaxic injection of an adeno-associated virus (AAV) expressing *LARGE* shRNA with GFP. A theta-patterned stimulation protocol readily induced long-lasting hippocampal CA1 LTP in control mice, but not in *LARGE* KD mice (Fig. 3*A*). Despite this LTP impairment, *LARGE* KD exhibited dramatic increases in field excitatory postsynaptic potential (fEPSP) amplitudes (Fig. 3*A*), leading us to analyze these amplitudes at different stimulation intensities. In an input-output analysis, the AMPA-R fEPSP amplitudes in *LARGE* KD mice increased significantly over input intensities of 30–100 mV (*SI Appendix*, Fig. S5*A*), However, *LARGE* KD did not affect presynaptic neurotransmitter release and short-term plasticity (STP), which were evaluated using the paired-pulse ratio (PPR). The PPRs at interpulse intervals of 200, 100, 75, 50, and 25 ms did not differ between control and *LARGE* KD mice (*SI Appendix*, Fig. S5*B*), suggesting that the synaptic changes observed in the latter mice are not presynaptic events.

The above results strongly suggest that *LARGE* KD increases the synaptic current by increasing the number of AMPA-R molecules at the postsynapses. Indeed, our analysis of miniature excitatory postsynaptic currents (mEPSCs) demonstrated that *LARGE* KD significantly increased the amplitude, but not the frequency, of mEPSCs relative to the controls (Fig. 3*B*). However, when we tested the effect of *LARGE* KD on inhibitory synapses, we observed no change in the miniature inhibitory postsynaptic current in either *LARGE* KD or rescue cells (*SI Appendix*, Fig. S6), consistent with the findings of a previous study (16). These electrophysiological analyses therefore demonstrate that changes in LARGE expression specifically affect the number of synaptic AMPA-R molecules at the excitatory postsynapses, without affecting presynapses or inhibitory synapses.

Next, we subjected cultured hippocampal neurons to confocal imaging to demonstrate that the number of GluA1 molecules within the dendritic spine increased significantly with *LARGE* KD relative to control neurons, and this increase was reversed by *LARGE* rescue (Fig. 3*C*). Finally, our biochemical analysis demonstrated that GluA1 expression in the postsynaptic density increased significantly in the hippocampi of *LARGE* KO mice relative to controls (*SI Appendix*, Fig. S7).

Together, the impaired hippocampal LTP (Fig. 3*A*) observed with *LARGE* KD is probably attributable to postsynaptic AMPA-R overload (Fig. 3 *B* and *C* and *SI Appendix*, Fig. S7), which inhibits the further capacity to increase the synaptic AMPA-R pool during LTP. Altogether, our results from those imaging, biochemistry, and electrophysiology experiments (Figs. 1–3) strongly support our working model, wherein LARGE negatively regulates AMPA-R trafficking from the Golgi to the plasma membrane, thus down-regulating AMPA-R synaptic targeting (Fig. 3*D*).

LARGE Deficiency Impairs Fear Memory. The effects of *LARGE* KD on AMPA-R trafficking and synaptic plasticity (LTP), which underlie learning and memory in the brain, strongly suggested a role for LARGE in cognitive functions in the brain. To determine whether LARGE deficiency could cause learning and memory problems in animals, we subjected *LARGE* KO ($Large^{myd-/-}$), wild-type, and heterozygous mice ($Large^{myd+/+}$ and $^{+/-}$) to Pavlovian fear conditioning (Fig. 4*A*) and observed similar freezing behaviors in all three groups (Fig. 4*B*). One day after fear conditioning, the mice were subjected to tests of contextual memory, an index of associative memory dependent on both hippocampal and amygdala function, and cued memory, a hippocampus-independent index of associative memory that still relies on proper amygdala function (17). Compared with wild-type mice, KO mice displayed significant reductions in freezing behavior during both contextual and cued memory tests (Fig. 4 *C* and *D*), indicating that *LARGE* KO leads to deficits in both hippocampus- and amygdala-dependent memory.

We note, however, that KO mice are constitutive mutants. Therefore, the observed memory deficits may be attributable to abnormal brain development. Accordingly, we knocked down *LARGE* in the bilateral hippocampal CA1 regions of adult mice and rats via the stereotaxic injection of an AAV expressing *LARGE* shRNA with GFP before Pavlovian fear conditioning to examine the potential effects of LARGE on memory processes in the absence of life-long inherent developmental abnormalities. Another group of mice injected with AAV expressing scrambled shRNA with GFP served as a control. We subsequently validated the efficacy of shRNA-mediated *LARGE* KD in vivo (*SI Appendix*, Fig. S8) and confirmed the reliability of the experimental animals used in fear tests (*SI Appendix*, Fig. S9). Although the two groups exhibited similar freezing behavior (Fig. 4*E*), *LARGE* KD mice exhibited significantly less freezing behavior during contextual but not cued memory tests (Fig. 4 *F* and *G*). In rats, *LARGE* KD in the hippocampal CA1 produced the same effects on memory (Fig. 4 *H*–*J*).

Discussion

Here, using a multidisciplinary approach, we obtained several lines of evidence that consistently and strongly support our hypothesis that LARGE down-regulates the cell-surface localization, and thus synaptic targeting, of AMPA-R by modulating AMPA-R trafficking from the Golgi to the plasma membrane. Moreover, increasing synaptic AMPA-R by knocking down LARGE occluded hippocampal LTP in vivo, resulting in a significant deficit in associative memory. Therefore, LARGE regulation of AMPA-R trafficking ultimately regulates memory. Given that LARGE mutations are linked to intellectual disabilities, this regulation of AMPA-R trafficking, as well as memory by LARGE, provides insight into the pathophysiology of neurological and psychiatric disorders associated with intellectual disability.

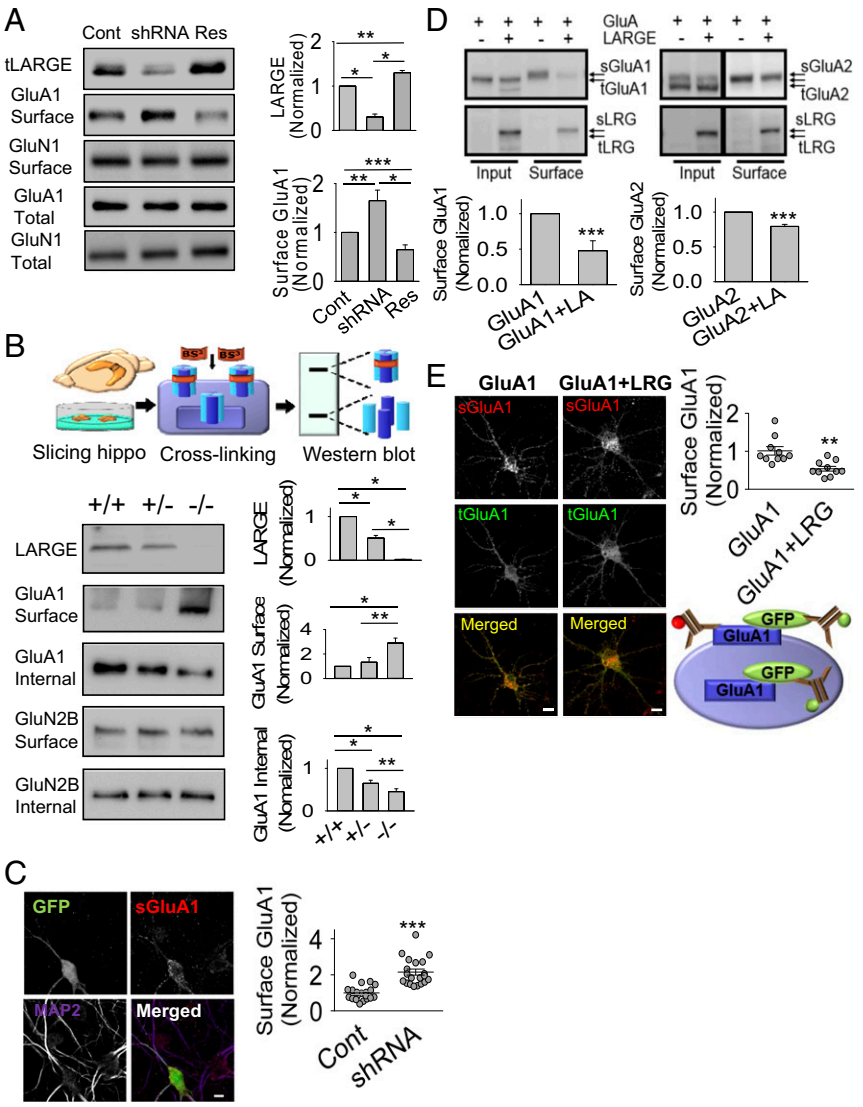

Fig. 2. LARGE down-regulates the surface localization of AMPA-R. (*A*) *LARGE* KD (shRNA) increased cell-surface GluA1 (Surface) expression, which was reversed by *LARGE* rescue (Res). However, changes in LARGE expression did not affect the total GluA1 or GluN1 expression ($n = 3$; one-way ANOVA: $^{*}P < 0.05$, $^{**}P < 0.01$, $^{***}P < 0.001$). (*B*) Schema of the ex vivo cross-linking of surface proteins using bis(sulfosuccinimidyl) suberate. Cross-linked and non–cross-linked proteins are indicated by high-molecular-weight bands (Surface) and low-molecular-weight bands (Internal), respectively. Surface GluA1 levels increased and internal GluA1 levels decreased in homozygous ($^{-/-}$) mice (*Large*^{myd}) ex vivo, compared with wild-type ($^{+/+}$) and heterozygous ($^{+/-}$) mice. GluN2B was used as a control ($n = 3$; two-tailed *t* test: $^{*}P < 0.05$, $^{**}P < 0.01$). (*C*) Imaging analysis of cultured neurons revealed higher levels of surface-localized GluA1 (sGluA1) in neurons expressing *LARGE* shRNA (GFP-positive neurons) than in neighboring GFP-negative neurons (Cont). The GluA1 antibody was applied before neuron permeabilization. MAP2, a marker of neuronal dendrites, was used to determine the number and morphology of neurons ($n = 20$, 20 neurons; Mann–Whitney rank-sum test: $^{***}P < 0.001$). (Scale bars: 10 μm.) (*D*) Coexpression of LARGE-GFP (LARGE or LRG) with myc-GluA1 (GluA1) and myc-GluA2 (GluA2) in HEK293T cells significantly reduced the respective cell-surface localization of GluA1 (sGluA1) and GluA2 (sGluA2). However, total GluA1 (tGluA1) and GluA2 (tGluA2) levels in the Input were not significantly altered ($n = 8$; two-tailed *t* test: $^{***}P < 0.001$). sLRG, surface LARGE; tLRG, total LARGE. (*E*) Coexpression of LARGE (LRG) with GFP-GluA1 significantly reduced cell sGluA1 levels at cultured neurons. A schema of our imaging assay is shown. sGluA1 was labeled with a red fluorophore-conjugated anti-GluA1 antibody before neuron permeabilization. After permeabilization, tGluA1 was stained using a green fluorophore-conjugated anti-GFP antibody ($n = 10$, 10 neurons; Mann–Whitney rank-sum test: $^{**}P < 0.01$). (Scale bar: 10 μm.)

Our previous mass spectrometry and Western blot analyses suggested a specific interaction of LARGE with AMPA-R in the brain (9). Our protein–protein interaction assays using HEK293T cells and ELISA (Fig. 1 *E*–*G*) confirmed the specific and direct interaction between the two proteins. HEK293T cells do not express synaptic proteins that might serve as intermediaries in the interaction of LARGE and AMPA-R. The ELISA was performed with purified proteins in vitro, which demonstrated that N-terminal ectodomain of AMPA-R binds to C-terminal ectodomain of LARGE. including two catalytic domains (CD1 and CD2) (Fig. 1 *F* and *G*). We could not narrow down the AMPA-R–binding domain of LARGE further since the truncation mutants of LARGE exhibit a totally different subcellular localization in HEK293T cells compared with wild-type LARGE (11). Since the protein purification yield of the CD1 or CD2 domain of LARGE was too low, probably due to low stability of the truncated proteins, the domains could not be used for the ELISA.

Although impaired LTP in hippocampal slices of *Large*$^{myd-/-}$ mice has been previously reported (8), this LTP occlusion is likely attributable to developmental defects in the hippocampus that result in abnormal neuronal migration, as reported by the same group (7, 18). In contrast, our study demonstrated the outcome of a LARGE deficit in adult animals, showing that memory deficits (Fig. 4 *E*–*J*), as

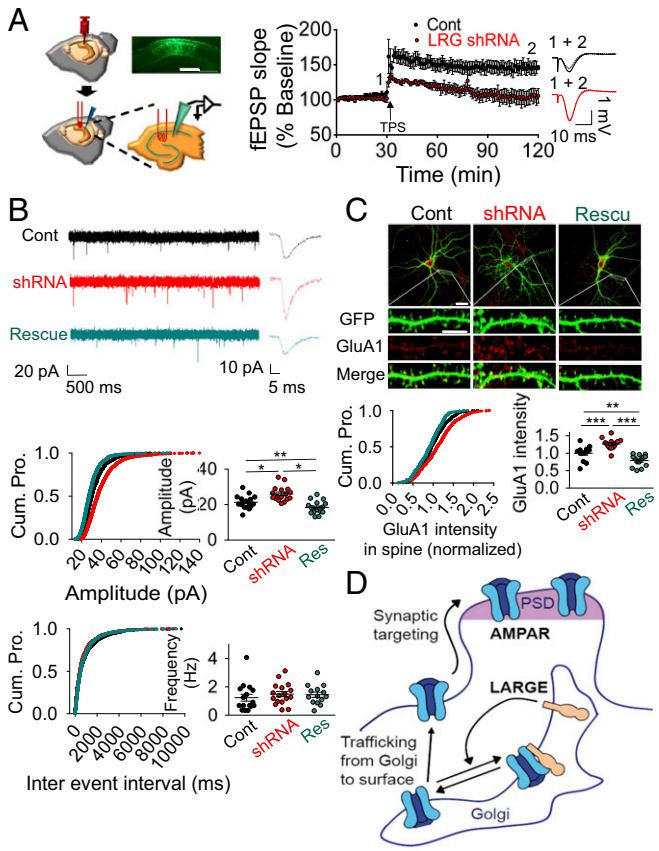

Fig. 3. *LARGE* KD causes synaptic AMPA-R overload, and thus impairs in vivo LTP in the hippocampal CA1 region. (*A*) Schema, plot, and traces from an in vivo LTP analysis after an injection of virus encoding *LARGE* shRNA. *LARGE* KD (LRG shRNA) was found to impair LTP (n = 8, eight mice; two-tailed *t* test: $P < 0.05$). Cont, control. (Scale bar: 300 μm.) (*B*) Whole-cell patch clamping yielded current traces, cumulative plots, and scattered plots from mEPSC analysis following transfection with plasmids encoding scrambled shRNA (Cont), *LARGE* shRNA, or *LARGE* rescue. *LARGE* KD increased the amplitude, but not the frequency, of mEPSCs, whereas *LARGE* rescue reversed this amplitude change. Three different groups from 48 coverslips in four batches of neuronal culture were recorded [n = 1,653, n = 1,660, and n = 1,622 events from n = 17, n = 17, and n = 17 neurons, respectively; Amplitude: $^*P < 0.001$, $^{**}P = 0.026$; Frequency: $P = 0.639$; Cont, black; shRNA, red; Rescue (Res), cyan]. Cum. Pro., cumulative probability. (*C*) *LARGE* KD (shRNA) increased the number of GluA1 molecules in the dendritic spines, whereas this phenomenon was reversed by *LARGE* rescue (n = 529, n = 529, and n = 562 spines from n = 13, n = 14, and n = 14 neurons, respectively; $^{**}P < 0.01$, $^{***}P < 0.001$). (Scale bars: whole-cell image, 30 μm; dendrite, 10 μm.) In an image of a neuron, the intensity of the GluA1 signal at the spine (synaptic GluA1) was normalized to the intensity of the GluA1 signal at the dendritic shaft (total GluA1). (*D*) Schema of our working model for the regulation of AMPA-R trafficking by LARGE. PSD, polysynaptic density. (*B* and *C*) One-way ANOVA was used.

well as occluded LTP (Fig. 3*A*), follow *LARGE* KD in the hippocampus. While the impaired LTP induction and deficits in memory make intuitive sense, the occlusion of LTP by increased surface and synaptic targeting of AMPA-R might seem paradoxical. However, consistent with our results, LTP occlusion due to elevation in postsynaptic AMPA-R surface localization and function was reported previously (19). Previous studies also have shown that abnormally increased synaptic activity impairs LTP and memory. For example, enhanced synaptic responses suppress LTP development, resulting in hippocampal memory deficits (20), whereas chronically increased fEPSPs cause persistent deficits in the acquisition of new spatial information (21, 22). Our electrophysiological (Fig. 3*B*), imaging (Fig. 3*C*), and biochemical (*SI Appendix*, Fig. S7) experiments consistently demonstrated that the number of synaptic AMPA-Rs is significantly increased by *LARGE* KD. Taken together, our results suggest that the overloading of synaptic AMPA-R caused by *LARGE* KD blocks further synaptic targeting of AMPA-R, resulting in occlusion of LTP. Therefore, consistent with previous studies, our study demonstrates that an appropriate balance between supply and removal of AMPA-R at synapses is necessary for normal LTP induction.

Our input-output analysis, in which the AMPA-R fEPSP amplitudes in *LARGE* KD mice increased significantly over all input intensities (*SI Appendix*, Fig. S5*A*), suggests a potentiated postsynaptic response by *LARGE* KD, leading to our hypothesis that *LARGE* KD increases the synaptic current by increasing the number of AMPA-R molecules at the postsynapses. On the other hand, the input-output change could be due to increased excitability of postsynaptic dendrites, as a result of a decreased threshold for action potential generation by alteration of dendritic ion channels. This phenomenon is known as EPSP-spike potentiation (23, 24). Thus, it is possible that LARGE may affect trafficking of ion channels involved in action potential generation.

In contrast to LTP induction, which was abrogated by *LARGE* KD, STP remained intact in *LARGE* KD mice (*SI Appendix*, Fig.

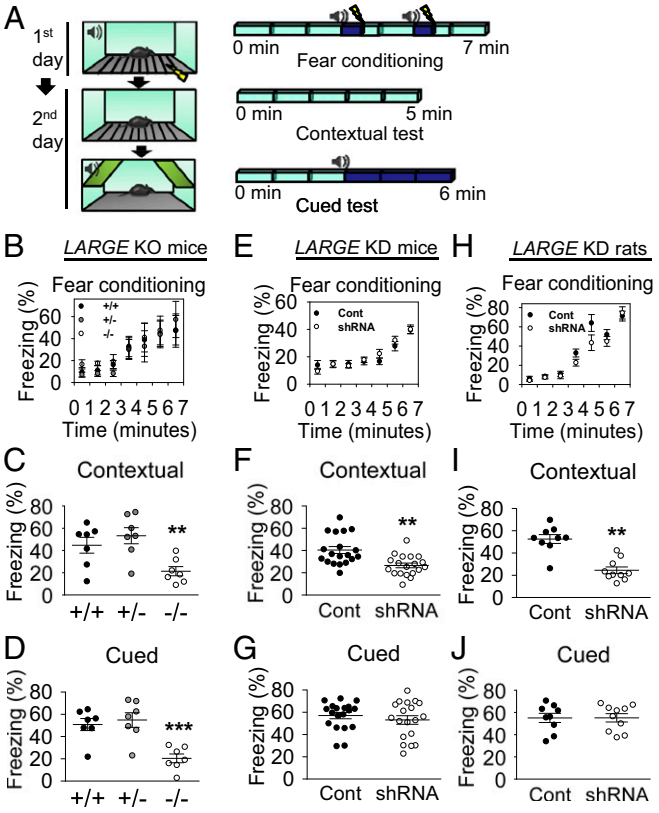

Fig. 4. LARGE deficiency impairs fear memory. (*A*) Schema of a fear memory test. (*B*) *LARGE* KO did not induce differences in fear conditioning (n = 7 mice, n = 7 mice, n = 7 mice). (*C* and *D*) Contextual and cued fear memory deficits were observed in KO mice ($^{-/-}$). (n = 7 mice, n = 7 mice, n = 7 mice; contextual, $^{**}P < 0.01$; cued, $^{***}P < 0.001$). (*E*) No differences in fear conditioning were observed in *LARGE* KD mice (n = 19, 19 mice). (*F*) Contextual memory deficits were observed in *LARGE* KD mice (n = 19, 19 mice; two-tailed *t* test: $^{**}P < 0.01$). (*G*) No differences were observed in cued memory (n = 19, 19 mice; Mann–Whitney rank-sum test: $P = 0.579$). (*H*) No differences in fear conditioning were observed in *LARGE* KD rats (n = 9, 10 rats). (*I*) Contextual memory deficits were observed in *LARGE* KD rats (n = 9, 10 rats; two-tailed *t* test: $^{**}P < 0.01$). (*J*) No differences were observed in cued memory (n = 9, 10 rats; two-tailed *t* test: $P = 0.987$). In *E*–*J*, animals were injected with a virus expressing either scrambled (Cont) or *LARGE* shRNA with GFP (shRNA). Two-way repeated measure ANOVA (*B*, *E*, and *H*) and one-way ANOVA (*C* and *D*) were used.

S5*B*), a result consistent with the normal acquisition of fear training in *LARGE* KO and *LARGE* KD animals (Fig. 4 *B*, *E*, and *H*). The fact that the STP was not changed by *LARGE* KD also supports our hypothesis that the effect of LARGE on synaptic plasticity is postsynaptic rather than presynaptic, as demonstrated by the absence of an effect of *LARGE* KD or overexpression on mEPSC frequency (Fig. 3*B*).

LARGE2 (GYLTL1B) is a homolog of LARGE (11) that, in principle, could compensate for the loss of LARGE (25). However, LARGE2 is not expressed in the brain (25), and is thus unlikely to compensate for the loss of LARGE in neuronal cultures or the brain. Our functional studies of LARGE also consistently suggest that the loss of LARGE in neurons is not compensated for by a homolog in the brain, at least in terms of LARGE function in AMPA-R trafficking and memory.

LARGE function in the brain has been studied by focusing on its association with the dystrophin glycoprotein complex (DGC) (7, 8, 16). However, the DGC, including dystroglycan, is specifically expressed in inhibitory GABAergic synapses and is not detected at excitatory glutamatergic synapses (16, 26). *LARGE* KD has no effect on inhibitory synaptic current (*SI Appendix*, Fig. S5), which is consistent with the findings of a previous study (16). In contrast, our study is focused on the function of LARGE in excitatory synapses where AMPA-Rs are expressed, which provided insight into the intellectual disability associated with *LARGE* mutations in patients with muscular dystrophy.

Intellectual disability refers to what used to be called "mental retardation," which is characterized by significant limitations in both intellectual functioning (intelligence quotient < 70) and adaptive behavior, as expressed in conceptual, social, and practical skills before the age of 18 y (27), and other cognitive deficits that are acquired throughout the lifespan (e.g., neurodegenerative-based dementia). Many X-linked brain disorders associated with intellectual disability are related to the proteins involved in the signaling pathways that support synaptic function (4). Fragile X syndrome, the most common form of inherited intellectual disability, is directly linked to the dysregulation of AMPA-R (28). Moreover, the intellectual disability-associated proteins PAK3 (p21 protein-activated kinase 3) and OPHN1 (oligophrenin 1) regulate the expression and stability of synaptic AMPA-R, respectively (29, 30). Furthermore, mutations in the GluA3 subunit of AMPA-R have been found in patients with X-linked intellectual disability (31). The nature of the alterations in AMPA-R trafficking and the manner in which these changes contribute to intellectual disability, however, remain largely unknown. In this regard, the regulation of AMPA-R trafficking and memory by the intellectual disability-associated protein LARGE demonstrated in this study provides useful clues for elucidating the pathophysiology underlying cognitive deficits in neurological and psychiatric disorders associated with intellectual disability.

Materials and Methods

Detailed experimental methods are described in *SI Appendix*. The use and care of animals in this study were performed in accordance with procedures approved by the Institutional Animal Care and Use Committee at the University of Texas Medical Branch and the Korea Advanced Institute of Science and Technology.

Preparation of cDNA, shRNA, and Viruses. LARGE expression vectors were kindly provided by Kevin Campbell, University of Iowa, Iowa City, IA. AAV constructs were designed, generated, and screened as previously described (details are provided in *SI Appendix*).

Animal Behavior Tests. Fear conditioning and fear memory tests were performed as described in *SI Appendix*.

Electrophysiological Analyses. Whole-cell voltage-clamping recordings of mEPSCs and in vivo fEPSP recordings were recorded as previously described (details are provided in *SI Appendix*).

ACKNOWLEDGMENTS. We thank Drs. Kevin P. Campbell and Richard L. Huganir for the generous gifts of cDNA plasmids, antibodies, and *Large*^{myd} mice. We thank all of the M.-G.K. laboratory members for technical assistance and advice in this study. This work was supported by the Institute for Basic Science (Grant R001-D1) and the University of Texas Medical Branch.

1. Peyrard M, et al. (1999) The human LARGE gene from 22q12.3-q13.1 is a new, distinct member of the glycosyltransferase gene family. *Proc Natl Acad Sci USA* 96:598–603.
2. Clarke NF, et al. (2011) Congenital muscular dystrophy type 1D (MDC1D) due to a large intragenic insertion/deletion, involving intron 10 of the LARGE gene. *Eur J Hum Genet* 19:452–457.
3. Longman C, et al. (2003) Mutations in the human LARGE gene cause MDC1D, a novel form of congenital muscular dystrophy with severe mental retardation and abnormal glycosylation of alpha-dystroglycan. *Hum Mol Genet* 12:2853–2861.
4. Vaillend C, Poirier R, Laroche S (2008) Genes, plasticity and mental retardation. *Behav Brain Res* 192:88–105.
5. Lisi MT, Cohn RD (2007) Congenital muscular dystrophies: New aspects of an expanding group of disorders. *Biochim Biophys Acta* 1772:159–172.
6. Holzfeind PJ, et al. (2002) Skeletal, cardiac and tongue muscle pathology, defective retinal transmission, and neuronal migration defects in the Large(myd) mouse defines a natural model for glycosylation-deficient muscle - eye - brain disorders. *Hum Mol Genet* 11:2673–2687.
7. Michele DE, et al. (2002) Post-translational disruption of dystroglycan-ligand interactions in congenital muscular dystrophies. *Nature* 418:417–422.
8. Satz JS, et al. (2010) Distinct functions of glial and neuronal dystroglycan in the developing and adult mouse brain. *J Neurosci* 30:14560–14572.
9. Kang MG, et al. (2012) Proteomic analysis of α-amino-3-hydroxy-5-methyl-4-isoxazole propionate receptor complexes. *J Biol Chem* 287:28632–28645.
10. Henley JM, Barker EA, Glebov OO (2011) Routes, destinations and delays: Recent advances in AMPA receptor trafficking. *Trends Neurosci* 34:258–268.
11. Brockington M, et al. (2005) Localization and functional analysis of the LARGE family of glycosyltransferases: Significance for muscular dystrophy. *Hum Mol Genet* 14:657–665.
12. Kanagawa M, et al. (2004) Molecular recognition by LARGE is essential for expression of functional dystroglycan. *Cell* 117:953–964.
13. Hall RA, Hansen A, Andersen PH, Soderling TR (1997) Surface expression of the AMPA receptor subunits GluR1, GluR2, and GluR4 in stably transfected baby hamster kidney cells. *J Neurochem* 68:625–630.
14. Okajima T, Xu A, Lei L, Irvine KD (2005) Chaperone activity of protein O-fucosyltransferase 1 promotes notch receptor folding. *Science* 307:1599–1603.
15. Lee DZ, Chung JM, Chung K, Kang MG (2012) Reactive oxygen species (ROS) modulate AMPA receptor phosphorylation and cell-surface localization in concert with pain-related behavior. *Pain* 153:1905–1915.
16. Pribiag H, Peng H, Shah WA, Stellwagen D, Carbonetto S (2014) Dystroglycan mediates homeostatic synaptic plasticity at GABAergic synapses. *Proc Natl Acad Sci USA* 111:6810–6815.
17. Sanders MJ, Wiltgen BJ, Fanselow MS (2003) The place of the hippocampus in fear conditioning. *Eur J Pharmacol* 463:217–223.
18. Michele DE, Campbell KP (2003) Dystrophin-glycoprotein complex: Post-translational process6ing and dystroglycan function. *J Biol Chem* 278:15457–15460.
19. Traunmüller L, Gomez AM, Nguyen TM, Scheiffele P (2016) Control of neuronal synapse specification by a highly dedicated alternative splicing program. *Science* 352:982–986.
20. Barnes CA, et al. (1994) LTP saturation and spatial learning disruption: Effects of task variables and saturation levels. *J Neurosci* 14:5793–5806.
21. Castro CA, Silbert LH, McNaughton BL, Barnes CA (1989) Recovery of spatial learning deficits after decay of electrically induced synaptic enhancement in the hippocampus. *Nature* 342:545–548.
22. McNaughton BL, Barnes CA, Rao G, Baldwin J, Rasmussen M (1986) Long-term enhancement of hippocampal synaptic transmission and the acquisition of spatial information. *J Neurosci* 6:563–571.
23. Bliss TV, Lomo T (1973) Long-lasting potentiation of synaptic transmission in the dentate area of the anaesthetized rabbit following stimulation of the perforant path. *J Physiol* 232:331–356.
24. Staff NP, Spruston N (2003) Intracellular correlate of EPSP-spike potentiation in CA1 pyramidal neurons is controlled by GABAergic modulation. *Hippocampus* 13:801–805.
25. Fujimura K, et al. (2005) LARGE2 facilitates the maturation of alpha-dystroglycan more effectively than LARGE. *Biochem Biophys Res Commun* 329:1162–1171.
26. Lévi S, et al. (2002) Dystroglycan is selectively associated with inhibitory GABAergic synapses but is dispensable for their differentiation. *J Neurosci* 22:4274–4285.
27. Kaufman L, Ayub M, Vincent JB (2010) The genetic basis of non-syndromic intellectual disability: A review. *J Neurodev Disord* 2:182–209.
28. Bowie D (2008) Ionotropic glutamate receptors & CNS disorders. *CNS Neurol Disord Drug Targets* 7:129–143.
29. Boda B, et al. (2004) The mental retardation protein PAK3 contributes to synapse formation and plasticity in hippocampus. *J Neurosci* 24:10816–10825.
30. Nadif Kasri N, Nakano-Kobayashi A, Malinow R, Li B, Van Aelst L (2009) The Rho-linked mental retardation protein oligophrenin-1 controls synapse maturation and plasticity by stabilizing AMPA receptors. *Genes Dev* 23:1289–1302.
31. Wu Y, et al. (2007) Mutations in ionotropic AMPA receptor 3 alter channel properties and are associated with moderate cognitive impairment in humans. *Proc Natl Acad Sci USA* 104:18163–18168.